Failure Analysis of Heavy-Ion-Irradiated Schottky Diodes

Megan C. Casey[1], Jean-Marie Lauenstein[1], Edward P. Wilcox[2], Alyson D. Topper[2], Michael J. Campola[1], and Kenneth A. LaBel[1]

[1]NASA Goddard Space Flight Center, Code 561.4, Greenbelt, MD 20771
[2]AS&D, Inc., Seabrook, MD 20706

National Aeronautics and Space Administration

In this work, we use high- and low-magnitude optical microscope images, infrared camera images, and scanning electron microscope images to identify and describe the failure locations in heavy-ion-irradiated Schottky diodes.

Introduction

Over the past several years, GSFGC and other institutions have been discussing the susceptibility of Schottky diodes to destructive (and non-destructive) single-event effects (SEEs) [1-5]. During the course of this work, four responses were observed in the diodes during the heavy-ion irradiations, and they are shown below (Figs.1a-1d). The diodes used in this work come from diodes used on an instrument for a specific NASA mission. There were no radiation requirements for this mission for diodes, but NASA EEE-INST-002 specifies a 70% electrical derating in the reverse voltage for Schottky diodes. It was determined that the diodes would see as much as 82 V under the worst case conditions, and thus, these parts needed to be tested to determine their SEE sensitivity. The results of those tests and the subsequent failure analysis on the tested DUTs are presented in this paper.

Passing Radiation Responses

All Post-Irradiation Parameter Measurements Within Specification

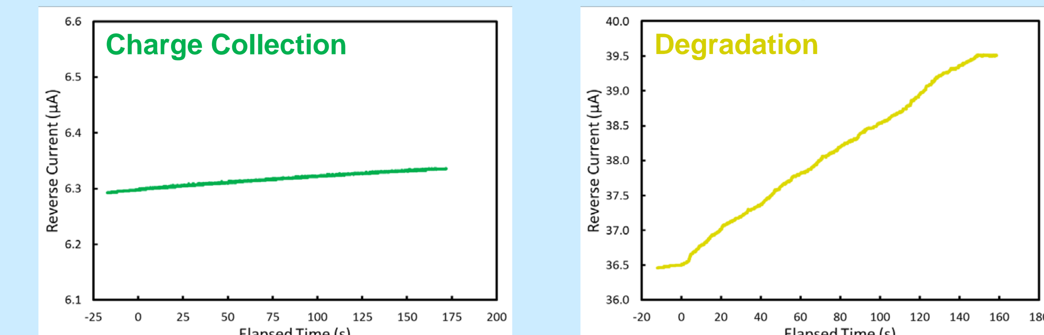

Fig. 1a. Charge collection is observed during the beam run. All post-irradiation parameters were within specification, and this was considered a passing condition

Fig. 1b. Degradation is observed in the reverse current during the beam run. All post-irradiation parameters were within specification, and this was considered a passing condition.

Failing Radiation Responses

Post-Irradiation Parameter Measurements Outside Specification

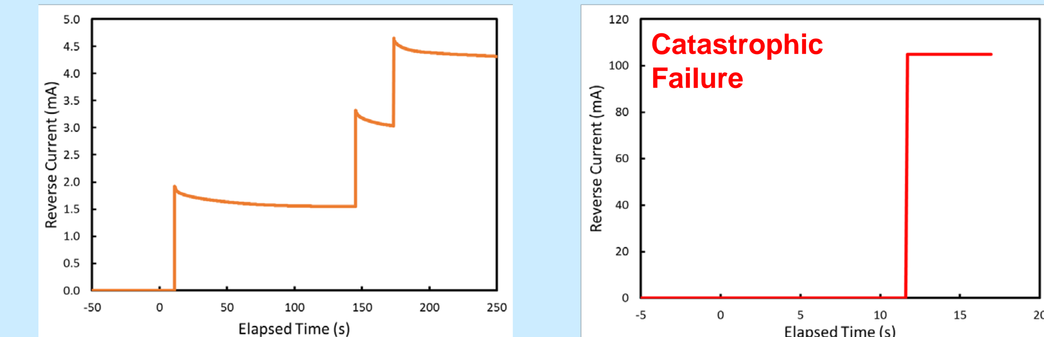

Fig. 1c. Degradation is observed in the reverse current during the beam run. Some or all of the post-irradiation parameters were outside of their specification, and this was considered a failing condition.

Fig. 1d. Some time after the beam is turned on, the anode and cathode short causing catastrophic failure. Some or all of the post-irradiation parameters were outside of their specification, and this was considered a failing condition.

Parts Analyzed in This Work

The diodes analyzed in this work were 1N6843s from two different manufacturers, Microsemi and International Rectifier (IR). These parts are dual (common cathode) Schottky diodes with a reverse voltage rating of 100 V and a forward current rating of 10 A. The Microsemi parts were qualified to the JANTXV standard, while the IR parts were qualified to JANS. The qualification standard should have no effect on the radiation response, but it is mentioned here for completeness, and to indicate, that while these parts are functionally the same, there are differences in the manufacturing that could (and did) lead to different radiation responses.

Table I: Device Information

Manufacturer	Serial Number	Ion Species	Failing Voltage	Radiation Response
Microsemi	SN5	1470 MeV Pr LET = 60 MeV-cm^2/mg	95 V	Catastrophic Failure
Microsemi	SN2	1858 MeV Ta LET = 79 MeV-cm^2/mg	65 V	Degradation and Failure
International Rectifier	SN7	1858 MeV Ta LET = 79 MeV-cm^2/mg	95 V	Catastrophic Failure

Catastrophic Failure – SN5

Up to the 65-V irradiation, only charge collection was observed (Fig. 2). When biased at 70 V, small increases in the reverse current (I_R) were observed during the beam run; however, the post-irradiation electrical parameter measurements all remained within specification.

During the 95-V irradiation, a small amount of degradation was observed almost immediately, but, within seconds, catastrophic failure was observed, meaning the anode and cathode shorted and the current was limited by the compliance settings on the power supply.

Fig. 2. Reverse currents from the power supply during each run. The reverse voltage at which the DUT was biased is shown in the legend.

The reverse I-V curve (Fig. 3a) shows that the part was degrading slightly during each run, however, after the 95-V run, I_R exceeded the 10 µA specification at less than 1 V. There was also a significant change in the forward I-V curve (Fig. 3b) after this run as well.

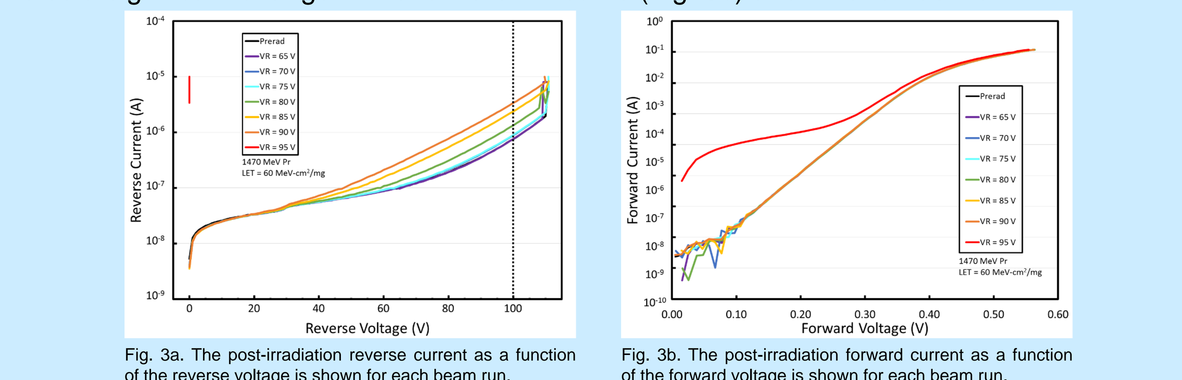

Fig. 3a. The post-irradiation reverse current as a function of the reverse voltage is shown for each beam run.

Fig. 3b. The post-irradiation forward current as a function of the forward voltage is shown for each beam run.

After irradiation, SN5 was examined using an IR camera and pictures were taken with a small voltage applied.

Bright white spot (indicating elevated temperature, and shown in Fig. 4a) just below the wirebond contact is the location of the failure.

Low-magnification (Fig. 4b) and high-magnification (Fig. 4c) optical images of the surface of the DUT did not show anything unusual at the location identified in the IR image.

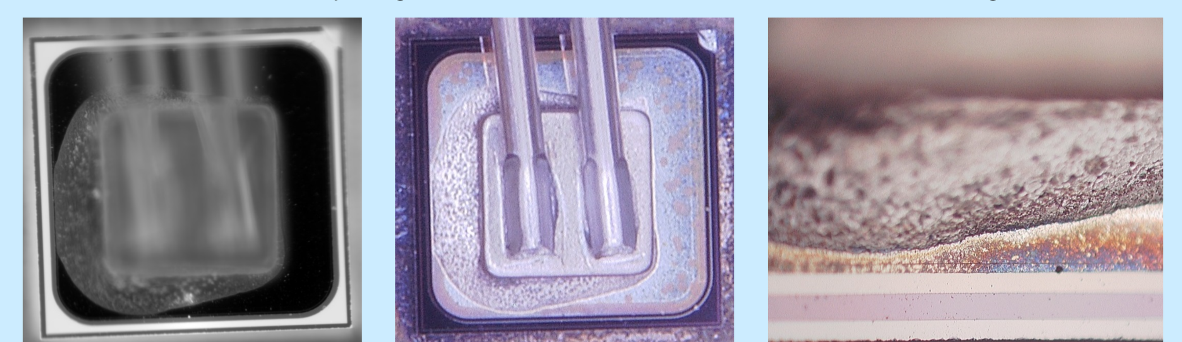

Fig. 4a. Thermal image of the irradiated DUT identifies location of failure.

Fig. 4b. The failure location is not visible in the low-magnification optical image of SN5.

Fig. 4c. The failure location is not visible in the high-magnification optical image of the DUT.

The DUT was then cross-sectioned at the location of the failure identified in the IR image, and then silicon was stained. A high-magnitude optical image (Fig. 5a) and a scanning electron microscope (SEM) image (Fig. 5b) of the failure are shown below.

The failure location is clearly observed from the Schottky barrier metal down through the epitaxial layer (epilayer), all the way to the bulk silicon. The extreme heat generated by the single-event strike also resulted in mechanical stress on the die and the subsequent cracking.

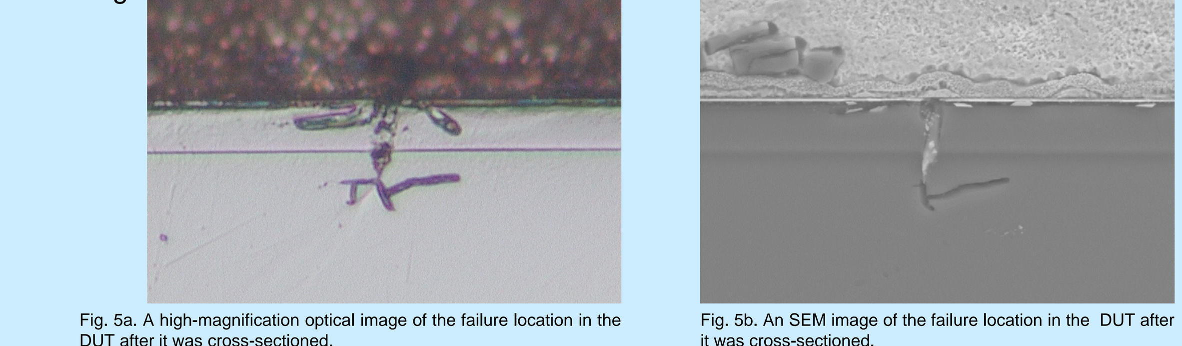

Fig. 5a. A high-magnification optical image of the failure location in the DUT after it was cross-sectioned.

Fig. 5b. An SEM image of the failure location in the DUT after it was cross-sectioned.

The failure created a void that was filled with displaced melted metal from the Schottky contact. The empty column generated during the failure is reminiscent of the filament that develops between the gate and the substrate through the neck region in power MOSFETs [8]

An element map, generated from energy dispersive x-ray spectroscopy (EDS), shows the displaced metal (Fig 6).

Fig. 6. Element map of the failure location in the DUT generated from EDS.

Degradation and Failure – SN2

Only charge collection was observed up to the 55-V irradiation.

When biased at 60 V, a ~60 nA increase in I_R was observed during the run.

All post-irradiation parameter measurements remained within specification.

At 65 V, however, SN2 experienced 100s of nA in degradation and the post-irradiation I_R measurement was out of specification.

Like SN5, the reverse I-V curve shows that the part was degrading slightly during each run.

After degradation was observed during the 65-V run, I_R exceeded 10 µA at less than the minimum rated 100 V (shown in Fig. 8a). No change in the forward I-V curve was observed (Fig. 8b).

Fig. 7. Reverse currents from the power supply during each run. The reverse voltage at which the DUT was biased is shown in the legend.

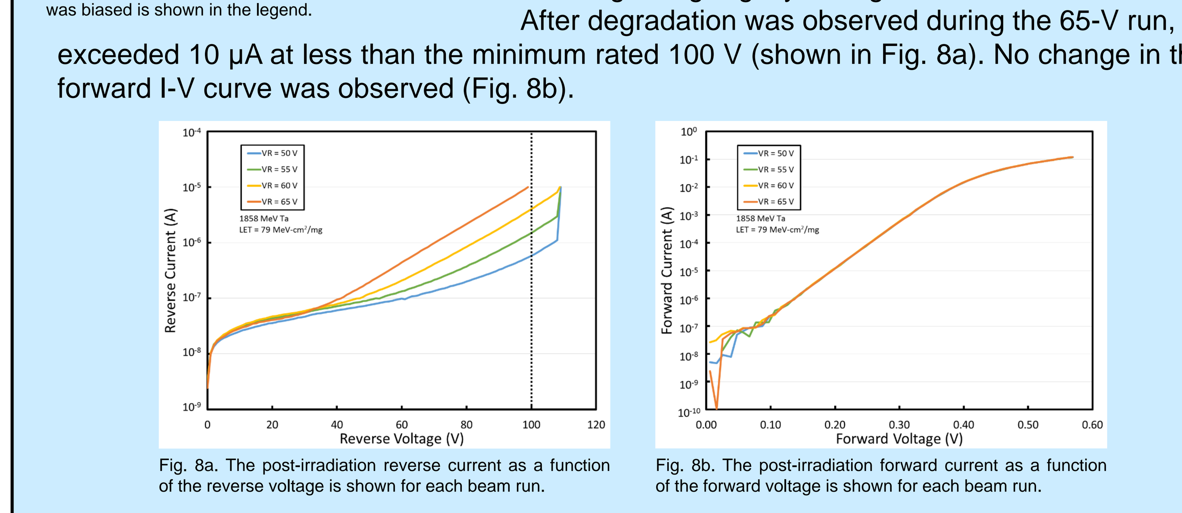

Fig. 8a. The post-irradiation reverse current as a function of the reverse voltage is shown for each beam run.

Fig. 8b. The post-irradiation forward current as a function of the forward voltage is shown for each beam run.

For SN2, even with 100 V applied, no failure locations were observed in the IR images (Fig. 9a), nor were any observed in the low-magnification optical images (Fig. 9b).

A different approach was then taken, where the bond wires, bond pad, and Schottky barrier metal were chemically etched and removed (Fig. 9c). On the surface of the silicon, a few discolorations were observed (Fig. 9d is an SEM of two of the discolorations), and under high-magnification, a fused particle, which was later determined to be silicon, was observed in the center of the discolorations (Fig. 9e).

The silicon particles (Fig. 9f) are roughly 1 µm across at the widest point.

Fig. 9a. Thermal image of the irradiated SN2 does not identify any failure locations.

Fig. 9b. No failure location is visible in the low-magnification optical image of the DUT.

Fig. 9c. Three discolorations are observed in the silicon of SN2 after the Schottky barrier metal, bond pad, and bond wires were removed.

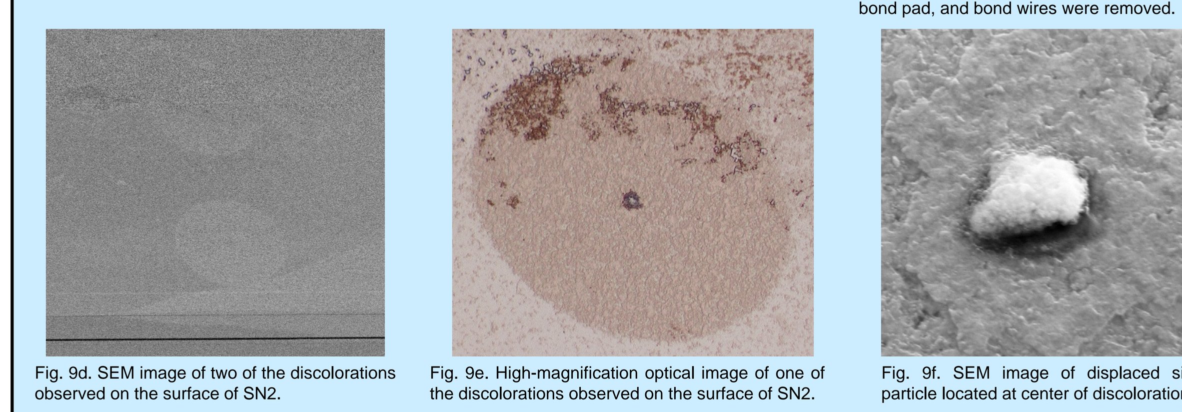

Fig. 9d. SEM image of two of the discolorations observed on the surface of SN2.

Fig. 9e. High-magnification optical image of one of the discolorations observed on the surface of SN2.

Fig. 9f. SEM image of displaced silicon particle located at center of discoloration.

Fig. 10. The DUT was cross-sectioned through one of the displaced silicon particles at the center of the discolored areas. No damage structure is present into the epilayer or bulk silicon.

After the discolored areas and displaced silicon locations were identified, the DUT was cross-sectioned and stained at one of these locations. The cross-section is shown on the left (Fig. 10), and no damage is observed beneath the fused silicon particle in the epilayer or silicon substrate. The lack of the column similar to that found in SN5 which shorted the anode and cathode and the fused particle on the surface of the silicon suggest that, rather than the event occurring at the epilayer/bulk silicon interface like in the DUT that experienced catastrophic failure, the damage occurred in SN2 at the Schottky metal/silicon interface.

Catastrophic Failure – SN7

Charge collection was observed on SN7 when biased at 75 and 80 V.

At 85 V and 90 V, a very small amount of degradation was observed (75 nA and 140 nA, respectively), but all post-irradiation electrical parameter measurements remained within specification.

During the 95-V irradiation, a very small increase in I_R was observed immediately after the beam was turned on, and then within seconds, the anode and cathode shorted, and again the current was only limited by the power supply.

Fig. 11. Reverse currents from the power supply for SN7 during each beam run. The reverse voltage at which the DUT was biased is shown in the legend.

Almost no degradation was observed in the reverse I-V curve (Fig. 12a) until the 95-V run when I_R exceeded the 10 µA specification at less than 1 V. Like with SN5, there was a significant change in the forward I-V curve (Fig. 12b) after the failing run.

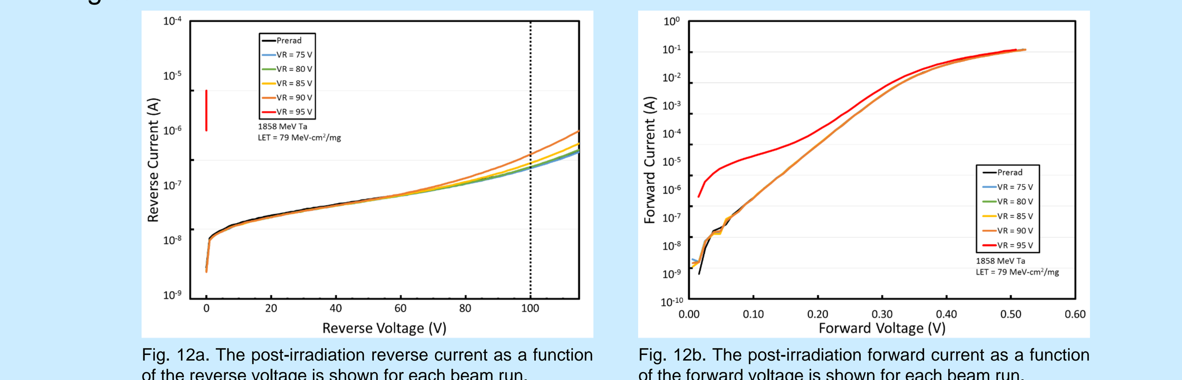

Fig. 12a. The post-irradiation reverse current as a function of the reverse voltage is shown for each beam run.

Fig. 12b. The post-irradiation forward current as a function of the forward voltage is shown for each beam run.

Using the thermal camera and a small applied voltage, the failure location was again visible in this DUT (Fig. 13a). When examined in the low-magnification optical image, the failure was not visible (Fig. 13b); however, when the magnification was increased, a dark spot could be seen (Figs. 13c and 13d). When that spot was investigated further with the SEM (Figs. 13e and 13f), it was clear that the Schottky barrier metal melted. Then, EDS showed (Fig. 13g) that not only had the metal melted, but silicon became displaced to the surface of the diode.

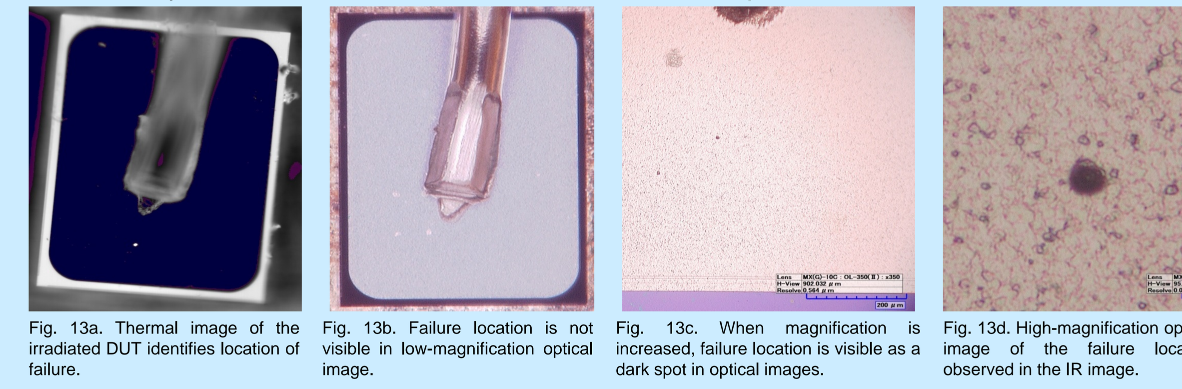

Fig. 13a. Thermal image of the irradiated DUT identifies location of failure.

Fig. 13b. Failure location is not visible in low-magnification optical image.

Fig. 13c. When magnification is increased, failure location is visible as a dark spot in optical images.

Fig. 13d. High-magnification optical image of the failure location observed in the IR image.

Fig. 13e. SEM image of the surface of SN7. Failure location is visible below the bondwire.

Fig. 13f. High-magnification SEM image of failure location.

Fig. 13f. Element map generated from EDS shows the Schottky barrier metal had melted away and silicon ball became displaced to the surface.

After identifying a failure location, SN7 was cross-sectioned at that location and stained (Fig. 14a). Like SN5, a large void was created through the silicon with most of the event occurring at the epilayer/bulk silicon border (Fig. 14b). There was a considerable portion at the silicon/metal interface as well. When EDS was performed on the cross-section, it was clear that, in addition to the displaced silicon that could be seen on the surface, aluminum from the Schottky barrier metal flowed into the bulk silicon (Fig. 14c).

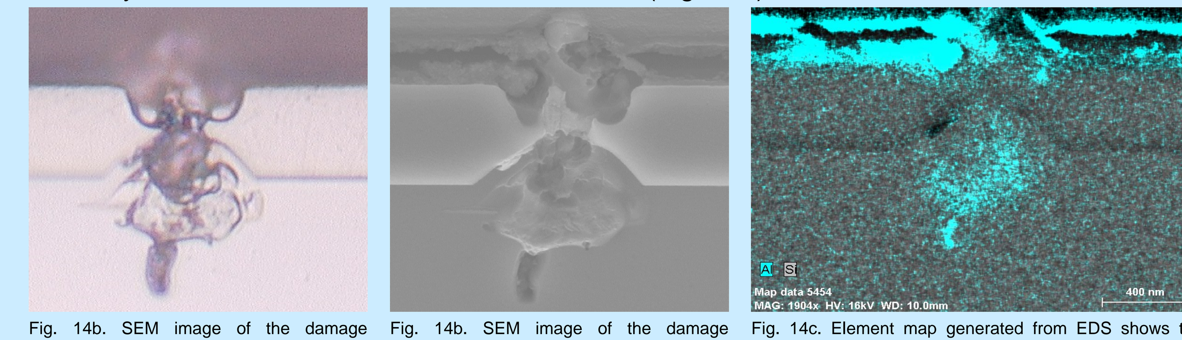

Fig. 14b. SEM image of the damage structure after the failure location in SN7 was cross-sectioned.

Fig. 14b. SEM image of the damage structure after the failure location in SN7 was cross-sectioned.

Fig. 14c. Element map generated from EDS shows the Schottky barrier metal migrated into the bulk silicon.

Conclusions

When a Schottky diode experiences enough degradation to cause the post-irradiation electrical parameter measurements to be out of specification, failure analysis appears to show that the damage occurs solely at the Schottky metal/silicon interface. This is in contrast to when a diode fails catastrophically. In that case, the event appears to also begin at the metal/silicon junction, however, the event generates such extreme heat that the materials become molten. A filament is then created that displaces the metal into the bulk silicon and can also displace silicon to the surface of the diode. This filament shorts the anode (bulk silicon) to the cathode (Schottky barrier metal) and the current is only limited by the power supply.

To avoid these radiation responses in which the diode is operating outside of the manufacturer's specifications, a reverse voltage derating of 50% is recommended when testing will not be conducted. If testing will be conducted on the flight diodes under the application-specific bias conditions, then a derating similar to power MOSFETs is recommended, in which the maximum reverse voltage that may be used is 75% of the last passing voltage.

Acknowledgment

The authors thank members of the NASA GSFC Part Analysis Lab (Code 562) without whom this work would not have been possible, especially Ron Weachock and Lang Hua, as well as Ray Ladbury (NASA GSFC REAG) for many informative conversations. Additionally, the authors would also like to acknowledge the personnel at TAMU for their support during beam runs. This work was supported by the NASA Electronics Parts and Packaging (NEPP) program and the Transiting Exoplanet Survey Satellite (TESS) program.

References

[1] M. C. Casey, J. M. Lauenstein, R. L. Ladbury, E. P. Wilcox, A. D. Topper and K. A. LaBel, "Schottky Diode Derating for Survivability in a Heavy Ion Environment," in IEEE Transactions on Nuclear Science, vol. 62, no. 6, pp. 2482-2489, Dec. 2015.

[2] K. A. LaBel, M. V. O'Bryan, D. Chen, M. J. Campola, M. C. Casey, J. A. Pellish, J.-M. Lauenstein, E. P. Wilcox, A. D. Topper, R. L. Ladbury, M. D. Berg, R. A. Gigliuto, A. J. Boutte, D. J. Cochran, S. P. Buchner, and D. P. Violette, "Compendium of Single Event Effects, Total Ionizing Dose, and Displacement Damage for Candidate Spacecraft Electronics for NASA," 2014 IEEE Radiation Effects Data Workshop (REDW), Paris, 2014, pp. 1-12.

[3] M. V. O'Bryan, K. A. LaBel, D. Chen, M. J. Campola, M. C. Casey, J.-M. Lauenstein, J. A. Pellish, R. L. Ladbury, and M. D. Berg, "Compendium of Current Single Event Effects for Candidate Spacecraft Electronics for NASA," 2015 IEEE Radiation Effects Data Workshop (REDW), Boston, MA, 2015, pp. 1-9.

[4] M. V. O'Bryan, K. A. LaBel, C. M. Szabo, D. Chen, M. J. Campola, M. C. Casey, J.-M. Lauenstein, J. A. Pellish, and M. D. Berg, "Compendium of Single Event Effects Results from NASA Goddard Space Flight Center", to be publichsed in Radiation Effects Data Workshop (REDW), 2016 IEEE, 11-15 July 2016.

[5] J. S. George, R. Koga, R. M. Moision, and A. Arroyo, "Single Event Burnout Observed in Schottky Diodes," 2013 IEEE Radiation Effects Data Workshop (REDW), San Francisco, CA, 2013, pp. 1-8.

[6] JANTX1N6843CCU3 datasheet, available online: https://www.microsemi.com/document-portal/doc_download/8943-lds-0130-pdf.

[7] Available Beams, available online: https://cyclotron.tamu.edu/ref/beamlist.pdf.

[8] J. S. George, R. Koga, R. M. Moision and A. Arroyo, "Single Event Burnout Observed in Schottky Diodes," 2013 IEEE Radiation Effects Data Workshop (REDW), San Francisco, CA, 2013, pp. 1-8.

To be presented by Megan C. Casey at the Institute of Electrical and Electronics Engineers (IEEE) Nuclear and Space Radiation Effects Conference in New Orleans, LA from July 18-21, 2017.